It has been suggested that the conformation about the C-glycosyl bond in the selenazole nucleosides may be restricted. If this occurs in solution, it would be expected to influence the stereochemistry of binding of SAD and/or SMP to IMPd.[7] Such restrictions could also affect the binding of selenazofurin and its 5'-phosphate to the enzymes involved in SAD synthesis. The inactive α anomer may have the same conformational restrictions as the active drug. However, the overall configuration of the α anomer, hence the location of its potential hydrogen-bonding groups, will remain distinct from that of the β form. Thus, it is likely that α-selenazofurin is either not converted to α-SAD or, if converted, the α-dinucleotide analogue cannot bind IMPd.[7]

Although selenazofurin behaves in many ways like its thiazole analogue, there are clearly differences between the two compounds and their anabolites. SAD is approximately three times more effective than TAD in inhibiting IMPd and is produced in greater quantities by P388 cells.[1-3] Most interesting is the greater efficacy of selenazofurin vs. tiazofurin as an antiviral agent.[4] The differences in size and conformation between the thiazole and selenazole rings are probably not by themselves sufficient to account for the differences in activity observed between the two drugs. However, the selenazole ring is also more reactive than the thiazole moiety. It is, for example, more susceptible to electrophilic substitution at the 5-position and is cleaved more easily.[27,28] Such differences in chemical reactivity may well contribute to the variations seen in drug activity.

Acknowledgment. This research was supported by the National Institutes of Health through Grants GM 21589, RR 05539, CA 06927, and CA 09035 and through an appropriation by the Commonwealth of Pennsylvania.

Registry No. I, 83705-13-9; II, 83705-14-0; tiazofurin, 60084-10-8; α-tiazofurin, 61502-38-3.

Supplementary Material Available: Anisotropic thermal parameters and listings of observed and calculated structure amplitudes for both structures (Tables VIII and IX, respectively) (20 pages). Ordering information is given on any current masthead page.

(24) Streeter, D.; Witkowski, J.; Khare, G.; Sidwell, R.; Bauer, R.; Robins, R.; Simon, L *Proc. Natl. Acad. Sci. U.S.A.* **1973**, *70*, 1174-1178.
(25) Prusiner, P.; Sundaralingam, M. *Nature (London), New Biology* **1973**, *244*, 116-117.
(26) For an alternative mechanism, see: Goswami, B.; Borek, E.; Sharma, O.; Fujitaki, J.; Smith, R. *Biochem. Biophys. Res. Commun.* **1979**, *89*, 830-836.
(27) Bulka, E. In "Organic Selenium Compounds: Their Chemistry and Biology"; Klayman, D., Gunther, W., Eds.; Wiley-Interscience: New York, 1973; pp 470-478.
(28) Guglielmetti, R. *Chem. Heterocycl. Compd.* **1979**, *34* (*Part 3*), 239-248.
(29) Voet, D. *J. Am. Chem. Soc.* **1973**, *95*, 3763-3770.
(30) Brown, E.; Bugg, C. *Acta Crystallogr., Sect. B.* **1980**, *B36*, 2597-2604.
(31) Bondi, A. *J. Phys. Chem.* **1964**, *68*, 441.
(32) Close S···O contacts have recently been observed in two independent molecules of the xylofuranosyl analogue of tiazofurin. Goldstein, B.; Mao, D.; Marquez, V. In "Abstracts of Papers"; 189th National Meeting of the American Chemical Society, Miami, FL, 1985; in press.
(33) Burchenal, J.; Pancoast, T.; Carroll, A.; Elslager, E.; Robins, R. *Proc. Am. Assoc. Cancer Res.* **1984**, *25*, Abstract No. 1375.

Conformational Analysis of a Cyclic Pentapeptide by One- and Two-Dimensional Nuclear Overhauser Effect Spectroscopy

Martha D. Bruch,† Joseph H. Noggle,* and Lila M. Gierasch*

Contribution from the Department of Chemistry, University of Delaware, Newark, Delaware 19716. *Received July 17, 1984*

Abstract: Detailed conformational analysis of the cyclic pentapeptide cyclo(D-phenylalanyl-L-prolylglycyl-D-alanyl-L-prolyl) in chloroform was carried out by one- and two-dimensional proton nuclear magnetic resonance spectroscopy. Two-dimensional *J*-resolved and spin-echo correlated spectroscopy were performed in order to verify the previous proton line assignments obtained for this peptide. The solution conformation was determined from measurement of one- and two-dimensional nuclear Overhauser effects. Quantitative interproton distances were determined from the time dependence of transient nuclear Overhauser effects, and these distances were compared to those obtained from the buildup rate of cross-peak intensities in a series of two-dimensional nuclear Overhauser effect spectra obtained with different mixing times. There was excellent agreement between the distances obtained by the two methods, and both methods yielded interproton distances with an average uncertainty of 0.2 Å. Furthermore, striking agreement was observed between interproton distances obtained for the peptide in solution and those for the crystal structure of this peptide as solved by X-ray diffraction. This indicates that the crystal structure, which contains one transannular hydrogen bond in a β turn and one in a γ turn, is essentially retained in solution.

Proton nuclear magnetic resonance (NMR) spectroscopy is a powerful tool for investigating the solution conformation of peptides and proteins. While much information can be obtained from chemical shifts and coupling constants, one of the best tools for conformational analysis is the nuclear Overhauser effect (NOE).[1] Conventional (1-D) steady-state and transient NOE experiments have been applied extensively to the conformational analysis of peptides[2-5] and proteins,[6-10] and two-dimensional nuclear Overhauser effect (2-D NOE) spectroscopy has been used to study the general conformational features of peptides[11,12] and

† Present address: Polymer Products Department, Experimental Station 269, E. I. du Pont de Nemours & Co., Wilmington, DE 19898.

(1) Smith, J. A.; Pease, L. G. *CRC Crit. Rev. Biochem.* **1980**, *8*, 315.
(2) Balaram, P.; Bothner-By, A. A.; Dadok, S. *J. Am. Chem. Soc.* **1972**, *94*, 4015.
(3) Bothner-By, A. A.; Johner, P. E. *Biophys. J.* **1978**, *24*, 779.
(4) Williamson, M. P.; Williams, D. H. *J. Am. Chem. Soc.* **1981**, *103*, 6580.
(5) Roques, B. P.; Rao, R.; Marion, D. *Biochimie* **1980**, *62*, 753.
(6) Dubs, A.; Wagner, G.; Wüthrich, K. *Biochim. Biophys. Acta* **1979**, *577*, 177.

0002-7863/85/1507-1400$01.50/0

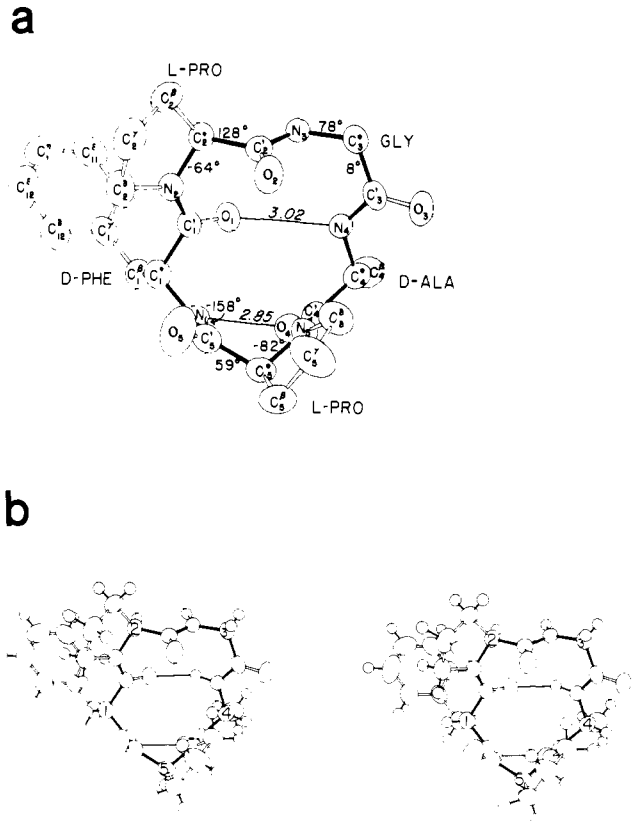

Figure 1. Structure of cyclo(D-Phe-Pro-Gly-D-Ala-Pro) as determined by X-ray diffraction.[21] (a) Diagram of the structure without hydrogens, showing labeling of atoms. (b) Stereoview of the structure with hydrogens.

proteins.[13-16] A semiquantitative relationship has been observed[17] between interproton distances in a molecule and the dependence of cross-peak intensities on the mixing time, τ_m, in a series of 2-D NOE spectra recorded with different mixing times. Apart from this, 2-D NOE spectroscopy has not been applied to the determination of quantitative interproton distances.

We report the determination of quantitative interproton distances from one- and two-dimensional NOE data on the cyclic pentapeptide cyclo(D-phenylalanyl-L-prolylglycyl-D-alanyl-L-prolyl)[cyclo(D-Phe-Pro-Gly-D-Ala-Pro)]. This cyclic pentapeptide is a convenient model compound for several reasons. It is a very rigid molecule and assumes a fixed conformation. Consequently, the interproton distances remain relatively constant in solution. In addition, the molecular motion can be characterized to a close approximation by a single correlation time describing the overall tumbling of the molecule. Therefore, the interpretation of NOE data in terms of interproton distances is greatly simplified.

Furthermore, this peptide is a good choice for detailed conformational analysis since the solution conformation has been studied previously.[18,19] The conformation of this peptide in solution contains all trans peptide bonds and is stabilized by two intramolecular hydrogen bonds, one in a β turn and one in a γ turn. These features can be characterized in detail by determination of quantitative interproton distances (for an illustration of the distances in these turns, see ref 20). Additionally, the single crystal structure of cyclo(D-Phe-Pro-Gly-D-Ala-Pro) has been determined by X-ray diffraction[21] (Figure 1). Consequently, the interproton distances obtained from NOE data in solution can be directly compared to distances obtained from X-ray data and the solution conformation can be compared to the single crystal conformation of this peptide. Good agreement is anticipated since previous studies (not based on NOE's) on this and a similar cyclic pentapeptide have suggested that the crystal conformations are essentially retained in solution.[18,19,21-24]

Theory

The theory of the NOE has been discussed in detail by Noggle and Schirmer.[25] The steady-state NOE, $\eta_i(j)$, is defined as the increase in the signal corresponding to spin i when j is saturated for a time which is long relative to the spin–lattice relaxation time. For two isolated spins i and j, the steady-state NOE is given by

$$\eta_i^{ss}(j) = \sigma_{ij}/\rho_i \quad (1)$$

In eq 1, σ_{ij} represents the cross-relaxation due to dipole–dipole interaction between spins i and j, and ρ_i represents the total relaxation of spin i, including mechanisms other than dipole–dipole relaxation with spin j. For a small molecule in the fast-motion limit, an appreciable NOE is only observed between two protons which are less than 3.0 Å apart.[8] However, the exact dependence of $\eta_i(j)$ on the interproton distance, r_{ij}, is not known in general because the exact nature of the relaxation mechanisms which contribute to ρ_i are not known. Quantitative interproton distances can be obtained by measuring the entire set of steady-state nuclear Overhauser effects in the molecule.[26] However, there are several limitations to this approach. Since $\eta_i(j)$ does not equal $\eta_j(i)$ in general,[25] two experiments must be performed for each interaction in the molecule. It is often not possible to measure both $\eta_i(j)$ and $\eta_j(i)$ for each interaction due to overlap of resonances in the proton NMR spectrum of a multispin system such as a cyclic peptide. Moreover, proton steady-state Overhauser effects in the fast-motion limit can have a maximum value of 0.50 and are generally considerably smaller than this. Small errors in the individual steady-state NOE values can result in large errors in the calculated distances. Another problem is that this method cannot readily be applied to molecules in the slow-motion limit due to the effects of spin diffusion.

Quantitative interproton distances can be obtained more easily from the buildup rate of the transient NOE.[6-10,27] In the simple case of two spins which relax exclusively via dipole–dipole interaction with each other, the transient NOE as a function of the preirradiation time is given by[10]

$$\eta_i(j) = (\sigma_{ij}/\rho_i)\{1 - \exp(-\rho_i t)\} \quad (2)$$

(7) Wagner, G.; Wüthrich, K. *J. Magn. Reson.* **1979**, *33*, 675.
(8) Braun, W.; Bosch, C.; Brown, L. R.; Go. N.; Wüthrich, K. *Biochim. Biophys. Acta* **1981**, *667*, 377.
(9) Olejniczak, E. T.; Poulsen, F. M.; Dobson, C. M. *J. Am. Chem. Soc.* **1981**, *103*, 6574.
(10) Dobson, C. M.; Olejniczak, E. T.; Poulsen, F. M.; Ratcliffe, R. G. *J. Magn. Reson.* **1982**, *48*, 97.
(11) Kessler, H.; Bermel, W.; Friedrich, A.; Krack, G.; Hull, W. E. *J. Am. Chem. Soc.* **1982**, *104*, 6297.
(12) Kessler, H.; Schuck, R.; Siegmeier, R. *J. Am. Chem. Soc.* **1982**, *104*, 4486.
(13) Wagner, G.; Kumar, A.; Wüthrich, K. *Eur. J. Biochem.* **1981**, *114*, 375.
(14) Wüthrich, K.; Wider, G.; Wagner, G.; Braun, W. *J. Mol. Biol.* **1982**, *155*, 311.
(15) Kumar, A.; Ernst, R. R.; Wüthrich, K. *Biochem. Biophys. Res. Commun.* **1980**, *95*, 1.
(16) Kumar, A.; Wagner, G.; Ernst, R. R.; Wüthrich, K. *Biochem. Biophys. Res. Commun.* **1980**, *96*, 1156.
(17) (a) Kumar, A.; Wagner, G.; Ernst, R. R.; Wüthrich, K. *J. Am. Chem. Soc.* **1981**, *103*, 3654. (b) Keepers, J. W.; James, T. L. *J. Magn. Reson.* **1984**, *57*, 404.
(18) Pease, L. G. In "Peptides: Structure and Biological Function, Proceedings of the Sixth American Peptide Symposium"; Gross, E., Meienhofer, J., Eds.; Pierce Chemical Co.: Rockford, IL, 1979; p 197.
(19) Bach, A. C.; Bothner-By, A. A.; Gierasch, L. M. *J. Am. Chem. Soc.* **1982**, *104*, 572.
(20) Rao, Ch. P.; Nagaraj, R.; Rao, C. N. R.; Balaram, P. *J. Am. Chem. Soc.* **1983**, *105*, 7423.
(21) Karle, I. L. In "Perspectives in Peptide Chemistry"; Eberle, A., Geiger, R., Wieland, T., Eds.; S. Karger: Basel, 1981; p 261.
(22) Pease, L. G.; Watson, C. *J. Am. Chem. Soc.* **1978**, *100*, 1279.
(23) Pease, L. G.; Watson, C. In "Peptides: Proceedings of the Fifth American Peptide Symposium"; Goodman, M., Meienhofer, J., Eds.; John Wiley: New York, 1977; p 346.
(24) Karle, I. L. *J. Am. Chem. Soc.* **1978**, *100*, 1286.
(25) Noggle, J. H.; Schirmer, R. E. "The Nuclear Overhauser Effect, Chemical Applications"; Academic Press: New York, 1971.
(26) Schirmer, R. E.; Noggle, J. H.; Davis, J. P.; Hart, P. A. *J. Am. Chem. Soc.* **1970**, *92*, 3266.
(27) Bothner-By, A. A.; Noggle, J. H. *J. Am. Chem. Soc.* **1979**, *101*, 5152.

However, in a multispin system such as a cyclic peptide, any one proton may relax via dipole–dipole interactions with several other protons, and the two-spin approximation given by eq 2 is not strictly valid. Dobson et al.[10] have shown that eq 2 is a good approximation if the following conditions are met:

(1) The effects of the cross-correlation[25] can be neglected. Dipole–dipole relaxation is caused by random motion of the relaxation vectors between pairs of spins. In a rigid molecule, the motion of one relaxation vector is correlated with the motions of other vectors. However, calculations indicate that these cross-correlation effects are generally small,[25] and it is a reasonable approximation to ignore them.

(2) $\sigma_{ij} > \sigma_{kj}$ for $k \neq i$, i.e., dipolar relaxation between spins i and j contributes more to the relaxation rate of spin j than the dipolar relaxation between spin j and any other spin. Physically, this means that proton j is closer to proton i than to any other proton.

(3) Sufficient irradiation power is used to cause the irradiated spin to be saturated essentially instantaneously.[27]

If these conditions are met, then σ_{ij} can be determined directly from a fit of transient NOE data to eq 2. Even if these conditions are not met the initial slope of $\eta_i(j)$ as a function of irradiation time can be used as an estimate of σ_{ij}.[6-10] Since σ_{ij} has a known dependence on the interproton distance r_{ij},[25] relative interproton distances can be calculated from the relative values of the cross-relaxation parameters. In particular, if all dipolar interactions in a molecule can be characterized by a single correlation time, then two relative interproton distances, r_{ij} and r_{kl}, can be calculated from σ_{ij} and σ_{kl} according to

$$r_{ij}/r_{kl} = (\sigma_{kl}/\sigma_{ij})^{1/6} \quad (3)$$

If the cross-relaxation parameter, σ_{mn}, is measured for two protons whose interproton distance, r_{mn}, is known, then other distances can be calculated relative to this known distance. Therefore, eq 3 can be used to obtain absolute interproton distances from cross-relaxation parameters measured from transient NOE data.

Although quantitative interproton distances can be obtained from one-dimensional transient NOE data, these experiments can be difficult to perform and interpret for several reasons. The major problem is the lack of selectivity of 1-D NOE experiments. It is difficult to apply enough power to saturate instantaneously one resonance without affecting neighboring resonances in a crowded spectrum. Also, small Overhauser effects are difficult to measure accurately in 1-D NOE difference experiments.[28] In addition, a separate set of 1-D transient NOE experiments must be performed for each interproton distance desired. Two-dimensional NOE spectroscopy eliminates these problems.

In this application, we used the 2-D NOE pulse sequence 90–t_1/2–90–τ_m – 90–t_1/2–t_2. The mixing time, τ_m, allows magnetization exchange due to dipole–dipole relaxation between two spins. A longer mixing time allows more dipole–dipole relaxation to occur. Hence, the intensities of the off-diagonal peaks are dependent on the length of the mixing time. In order to see off-diagonal peaks of appreciable intensity in a 2-D NOE spectrum, the mixing time must be of the order of magnitude of the spin–lattice relaxation time. The dependence of the off-diagonal peak intensities on the mixing time has been determined theoretically[29,30] and experimentally[17] by Ernst and co-workers. They showed that the initial buildup rate of the cross-peak intensity, $I_{ij}(\tau_m)$, is proportional to σ_{ij} according to[31]

$$I_{ij}(\tau_m)/I_{ii}(0) = \sigma_{ij}\tau_m \quad (4)$$

In eq 4, $I_{ii}(0)$ is the diagonal-peak intensity extrapolated to $\tau_m = 0$. This equation is an approximation that is only valid for short values of the mixing time. As in 1-D experiments, eq 3 can be used to calculate relative interproton distances from values of the cross-relaxation parameters determined from a series of 2-D NOE spectra obtained with different mixing times. It should be noted that cross-peaks due to J coupling can occur in 2-D NOE spectra obtained with short mixing times. However, these J cross-peaks can be distinguished from true NOE peaks since the intensity of J cross-peaks decreases exponentially with increasing mixing time.[31-33]

Experimental Section

Materials. cyclo-(D-Phe-Pro-Gly-D-Ala-Pro) was synthesized according to previously described methods.[22] Approximately 20 mg of the peptide was dissolved in 0.5 mL of $CDCl_3$, resulting in a concentration of 0.085 M. The solution was transferred to a previously constricted 5-mm NMR tube (Wilmad Glass Co.) and was degassed by several freeze–pump–thaw cycles on a high-vacuum line ($\sim 10^{-5}$ torr) to remove dissolved oxygen.

NMR Spectroscopy. All spectra were recorded with a Bruker WM 250 spectrometer equipped with an Aspect 2000 computer, operated in the Fourier transform mode with quadrature detection. The software used to obtain the two-dimensional NMR spectra was from Bruker Instruments, versions 801010 or 810515. A 16-cycle modification of the phase cycling routine Exorcycle was used to suppress signals due to pulse imperfections,[34] and a multiple of 16 transients was recorded for each t_1 value. The free induction decay of each 2-D NMR experiment was multiplied by a sine-bell function with zero phase and a period equal to twice the acquisition time in both dimensions. This improves resolution with less line shape distortion and less loss of signal-to-noise than traditional resolution enhancement routines.[35] Resolution enhancement was necessary since absolute value spectra were calculated in all cases.

Two-dimensional J-resolved (2-D J) data on cyclo(D-Phe-Pro-Gly-D-Ala-Pro) were acquired with use of sweep widths of ±34.4 Hz (64 t_1 values) in ω_1 and 2200 Hz (4096 data pts) in ω_2. Digital resolution after zero filling was 0.54 Hz/pt in both dimensions. A 4-s relaxation delay was used, and 16 transients were accumulated for each t_1 value. The total acquisition time was 3.5 h. Spin-echo correlated (SECSY) data on this peptide were acquired with sweep widths of ±1000 Hz (256 t_1 values) in ω_1 and 2000 Hz (512 data pts) in ω_2. Digital resolution after zero filling was 3.91 Hz/pt in both dimensions. A 6-s relaxation delay was used, and 16 transients were accumulated for each t_1 value. The total acquisition time was 9 h. The temperature was controlled at 300 K for both experiments.

All 2-D NOE experiments were performed with several mixing times. A relaxation delay of 8 s, greater than 5 times the longest T_1, was inserted between scans to ensure quantitative peak intensities. Sixteen transients were accumulated for each t_1 value, and the total acquisition time was 10 h per experiment. Since 2-D NOE employs a three-pulse sequence, a 16 cycle phase cycling routine does not completely eliminate artifacts in the 2-D NOE spectrum. In particular, large quadrature image peaks can arise if the offset frequency is placed in the center of the spectrum and quadrature detection is employed. To eliminate these quadrature image peaks and other noise, the offset frequency was placed at the left edge of the spectrum, and twice the normal sweep width was used in both dimensions. The data matrix was 4000 Hz (512 pts) in the ω_2 direction and ±2000 Hz (256 t_1 values) in the ω_1 direction. This gives a digital resolution of 7.81 Hz/pt in both dimensions after zero filling. The increment for the t_1 values was 0.125 ms, and the initial t_1 value was equal to this increment. The temperature was controlled at 303 K for all 2-D NOE experiments.

1-D NOE experiments were performed at 303 K in the difference mode. Sixteen transients were acquired with the second radio frequency field on-resonance of the spin to be saturated. Then sixteen transients were recorded off-resonance, and the total FID off-resonance was substracted from the total FID on-resonance. This cycle was repeated four times. The resultant difference spectrum was transformed and compared to a spectrum corresponding to 64 scans off-resonance. The NOE is the ratio of the intensity of the resonance in the difference spectrum to the intensity of the resonance in the off-resonance spectrum.

The decoupler power used was the minimum required to saturate instantaneously the spin of interest. If spin i is completely saturated, the intensity of the peak for spin i in the difference spectrum is $-M_o$. In this case, M_o is the intensity of spin i in the subtracted spectrum. This was

(28) Mersh, J. D.; Sanders, J. K. M. *J. Magn. Reson.* **1982** *50*, 289.
(29) Jeener, J.; Meier, B. H.; Bachmann, P.; Ernst, R. R. *J. Chem. Phys.* **1979**, *71*, 4546.
(30) Macura, S.; Ernst, R. R. *Mol. Phys.* **1980**, *41*, 95.
(31) Macura, S.; Wüthrich, K.; Ernst, R. R. *J. Magn. Reson.* **1982**, *47*, 351.
(32) Macura, S.; Huang, Y.; Suter, D.; Ernst, R. R. *J. Magn. Reson.* **1981**, *43*, 259.
(33) Macura, S.; Wüthrich, K.; Ernst, R. R. *J. Magn. Reson.* **1982**, *46*, 269.
(34) Bodenhausen, G.; Freeman, R.; Turner, D. L. *J. Magn. Reson.* **1977**, *27*, 511.
(35) DeMarco, A.; Wüthrich, K. *J. Magn. Reson.* **1976**, *24*, 201.

Table I. Chemical Shifts and Coupling Constants for Cyclo(D-Phe-Pro-Gly-D-Ala-Pro)

assignment	chemical[b] shift (ppm)	coupling[c] constants (Hz)
Phe NH	7.90	9.9
Ala NH	7.74	9.0
Gly NH	6.66	8.3, 5.6
aromatics	7.25	*a*
Pro-5 H^{α}	4.85	8.3, 2.1
Phe H^{α}	4.83	10.0, 8.3
Ala H^{α}	4.81	8.8, 7.0
Gly H^{α}	4.18	18.1, 7.6
Pro-2 H^{α}	3.97	7.0
Gly H^{α}	3.67	18.1, 6.0
Pro-2 H^{δ}	3.64	*a*
Pro-5 H^{δ}	3.35	*a*
Phe H^{β}	2.96	8.3
Pro-2 H^{δ}	2.67	*a*
Pro-5 H^{β}	2.43	*a*
Pro-5 H^{γ}	2.12	*a*
Pro-2 H^{γ}	1.98	*a*
Pro-2 H^{β}, Pro-5 H^{γ}	1.90	*a*
Pro-5 H^{β}	1.71	*a*
Pro-2 H^{γ}	1.42	*a*
Ala H^{β}	1.36	6.7

[a] Not first order—coupling constants cannot be measured. [b] Uncertainty associated with chemical shifts is ±0.01 ppm. [c] Uncertainty associated with coupling constants is ±0.3 Hz.

a practical criterion for complete saturation. A saturation time of 10 s, which was greater than eight times the longest T_1, was used for steady-state NOE experiments. Saturating power was turned off during acquisition so that coupled spectra were obtained. Quadrature detection was employed.

T_1 values were measured as a function of temperature with use of a $180°-\tau-90°$ inversion-recovery pulse sequence and a least-squares analysis of the integral data.

Results and Discussion

Proton Line Assignments. The 250-MHz proton NMR spectrum of cyclo(D-Phe-Pro-Gly-D-Ala-Pro) is shown in Figure 2. The line assignments were previously determined by Bach et al.[19] from high-resolution 600-MHz proton spectra. These assignments were confirmed by a combination of 2-D *J*-resolved and spin-echo correlated spectroscopy since the interpretation of the NOE data depends critically on the line assignments. These assignments, summarized in Table I, agree completely with those obtained by Bach et al. Furthermore, individual multiplets which are severely overlapped even at 600 MHz were resolved into individual subspectra by 2-D *J*-resolved spectroscopy, and the chemical shifts and coupling constants for these multiplets were measured directly from the *J*-resolved spectrum. For example, the three multiplets corresponding to Pro-5 H^{α}, Phe H^{α}, and Ala H^{α}, whose chemical shifts differ by only 0.02 ppm, were resolved in the 2-D *J*-resolved spectrum. The individual multiplets for these three protons are shown in Figure 3.

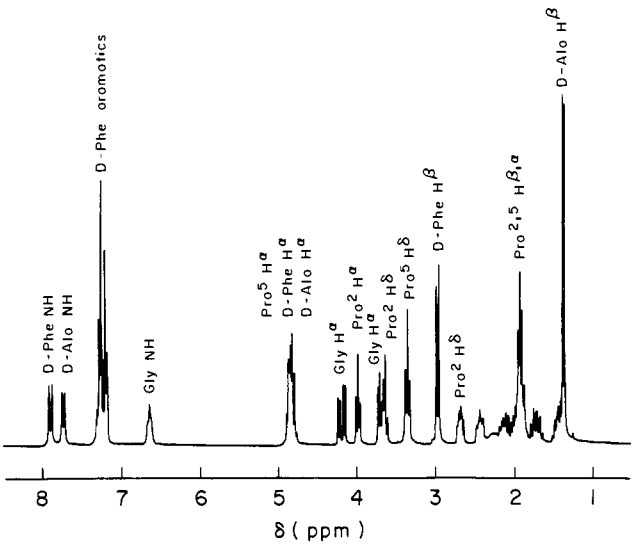

Figure 2. Proton NMR spectrum (250 MHz) of cyclo(D-Phe-Pro-Gly-D-Ala-Pro) in $CDCl_3$. Sixteen transients were recorded at 303 K. Peptide concentration 20 mg/0.5 mL.

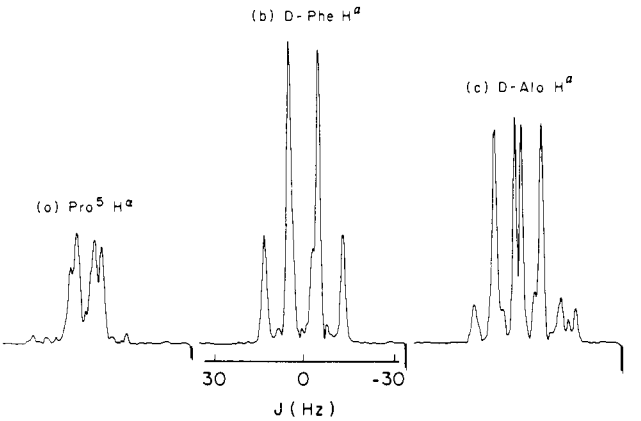

Figure 3. Cross sections of the α region of the tilted 2-D *J*-resolved spectrum of cyclo(D-Phe-Pro-Gly-D-Ala-Pro) in $CDCl_3$. These cross sections cover a range of ±34.4 Hz along the *J* axis and are taken through chemical shifts corresponding to (a) Pro-5 H^{α}, (b) Phe H^{α}, and (c) Ala H^{α}.

Spin–Lattice Relaxation Times. The proton spin–lattice relaxation times as a function of temperature for cyclo(D-Phe-Pro-Gly-D-Ala-Pro) in chloroform are summarized in Table II. All proton T_1 values decrease with decreasing temperature and start to level off at about 227 K. This implies that the molecule in chloroform is in the fast-motion limit throughout this temperature range. The T_1 values of all protons appear to reach a minimum at approximately the same temperature, and there was

Table II. Proton T_1 Values as a Function of Temperature, for Cyclo(D-Phe-Pro-Gly-D-Ala-Pro) in $CDCl_3$

spin	chemical shift at 300 K	T_1[a,b] at 303 K	T_1[a,c] at 283 K	T_1[a,c] at 264 K	T_1[a,c] at 243 K	T_1[a,c] at 227 K
Phe NH	7.90	0.63	0.47	0.37	0.31	0.29
Ala NH	7.74	0.74	0.53	0.42	0.35	0.32
Gly NH	6.66	0.46	0.33	0.27	0.23	*d*
Gly H^{α}	4.18	0.51	0.35	0.29	0.24	0.22
Gly H^{α}	3.67	0.36	0.33	0.27	0.21	0.21
Pro-2 H^{α}	3.97	0.91	0.66	0.55	0.43	0.41
Phe H^{β}	2.96	0.36	0.27	0.22	0.19	0.19
Ala H^{β}	1.36	0.50	0.39	0.28	0.21	0.17
Pro-5 H^{β}	2.43	0.45	0.34	0.29	0.25	0.25
Pro-5 H^{δ}	3.35	0.39	0.30	0.25	0.22	0.22
Pro-2 H^{δ}	3.64	0.36	0.32	0.26	0.21	0.20
Pro-2 H^{δ}	2.67	0.34	0.26	0.22	0.19	0.19

[a] Probe temperature calibrated from $\delta_{OH} - \delta_{CH_3}$ of neat methanol run at the same temperature. Uncertainty is ±1 K. [b] All T_1 values are in units of seconds. Uncertainty on T_1 values at 303 K is ±0.02 s. [c] All T_1 values are in units of seconds. Uncertainty on T_1 values at other temperatures is ±0.01 s. [d] Could not be measured.

Table III. Steady-State NOE Values for Protons in Cyclo(D-Phe-Pro-Gly-D-Ala-Pro)

spin i identity	spin i chemical shift	spin j identity	spin j chemical shift	$\eta_i^{ss}(j)^b$	$\eta_j^{ss}(i)^b$
Phe NH	7.90	Pro-5 H^α	4.85	0.09	0.18
Phe NH	7.90	Phe H^β	2.96	0.09	0.03
Ala NH	7.74	Gly NH	6.66	a	0.02
Gly NH	6.66	Pro-2 H^α	3.97	0.13	0.19
Gly NH	6.66	Gly H^α	3.67	0.06	0.04
Gly H^α	4.18	Gly H^α	3.67	0.28	0.24
Pro-2 H^δ	3.64	Pro-2 H^δ	2.67	0.28	0.26
Pro-2 H^δ	3.64	Phe H^α	4.83	0.07	0.12
Pro-5 H^δ	2.43	Ala H^α	4.81	0.04	0.21
Phe aromatics[c]	7.25	Pro-2 H^δ	2.67	0.04	0.02
Phe aromatics[c]	7.25	Phe H^α	4.83	0.02	0.04
Phe aromatics[c]	7.25	Phe H^β	2.96	0.10	0.04
Phe H^α	4.83	Phe H^β	2.96	0.08	0.03
Ala H^α	4.81	Ala H^β	1.36	0.16	0.02
Pro-2 H^γ	1.98	Pro-2 H^γ	1.42	0.18	0.13
Pro-5 H^β	2.43	Pro-5 H^β	1.71	0.30	0.27

[a] NOE was less than 0.02. [b] Uncertainties on $\eta_i^{ss}(j)$ and $\eta_j^{ss}(i)$ are ±0.02. [c] The calculated values for the aromatic ring assume the two ortho protons are involved in the interaction.

no sign of more than one recovery rate in any of the inversion recovery curves. Both of these results indicate that, in chloroform, the molecule can be characterized by a single correlation time which describes the overall tumbling of the molecule. This conclusion is further supported by ^{13}C relaxation times obtained for this peptide. When corrected for the number of directly bonded protons, spin–lattice relaxation times for all carbons are approximately the same. Carbon-13 relaxation times range from 0.49 s for Phe C^α to 0.75 s for one of the aromatic ring carbons. If dipole–dipole relaxation with directly bonded protons is assumed to be the dominant mechanism, then a correlation time of 8×10^{-11} s can be calculated from the average ^{13}C T_1 value of 0.62 s.

It should be noted that the glycine amide proton has a shorter relaxation time (0.46 s at 303 K) than either the phenylalanine or alanine amide protons (0.63 and 0.74 s, respectively). Phe NH and Ala NH are involved in intramolecular hydrogen bonds, but Gly NH is exposed to the solvent.[18,23] Consequently, additional relaxation mechanisms (e.g., exchange with residual water) may be available to Gly NH which are not available to Phe NH and Ala NH.

Steady-State Overhauser Effects. Steady-state Overhauser effects were measured at 303 K for cyclo(D-Phe-Pro-Gly-D-Ala-Pro) in chloroform in order to determine which interactions to study in detail. These results are summarized in Table III, and the corresponding difference spectra are shown in Figure 4. The saturated resonance, indicated by an arrow, gives rise to a large negative peak in the difference spectrum.

The top trace in Figure 4 is the null experiment corresponding to the difference between two off-resonance spectra decoupled at different frequencies. The dispersion mode peaks corresponding to a zero NOE can be seen in this spectrum.

Phe NH is saturated in Figure 4b. A small NOE (3%) is observed between Phe NH and the Phe H^β's, and a larger effect (18%) is observed between Phe NH and one of the overlapped H^α resonances. A priori, one might expect this peak to represent an NOE between the Phe NH and Phe H^α. Comparison of the observed pattern in the difference spectrum to 2-D J cross sections shown in Figure 3 reveals this interaction to be between the Phe NH and the Pro-5 H^α, not Phe H^α. This NOE indicated that the H^α of Pro-5 is spatially close to the amide proton of phenylalanine. This, in turn, is evidence for the existence of a γ turn involving Ala, Pro-5, and Phe with an intramolecular hydrogen bond between Phe NH and the carbonyl of Ala. This supports the previous conclusion that the crystal and solution conformations of this peptide are the same.[18,19,21]

Similarly, there is a large NOE (19%) observed between Gly NH and Pro-2 H^α when Gly NH is saturated. This is evidence for a type II β turn involving residues 1 to 4 (numbered as in Figure 1) and supports previous proposals for an intramolecular hydrogen bond between Ala NH and the carbonyl of phenylalanine.[18,21] There is a small NOE (4%) between Gly NH and the upfield Gly H^α resonance, but no NOE to the downfield Gly H^α. This indicates that the glycine amide proton is closer to one of the α-methylene protons (the upfield resonance) than to the other. This is consistent with interpretations of the arrangement of these protons based on vicinal coupling constants and chemical shift arguments (viz., the upfield Gly H^α is "anti" to the Pro C=O and is related by a dihedral angle of ~20° to the NH, yielding a smaller coupling constant than the other H^α which is nearly "syn" to the C=O and ~140° from the NH).

Since Pro-5 H^α, Phe H^α, and Ala H^α are severely overlapped, these resonances cannot be saturated individually. When all three

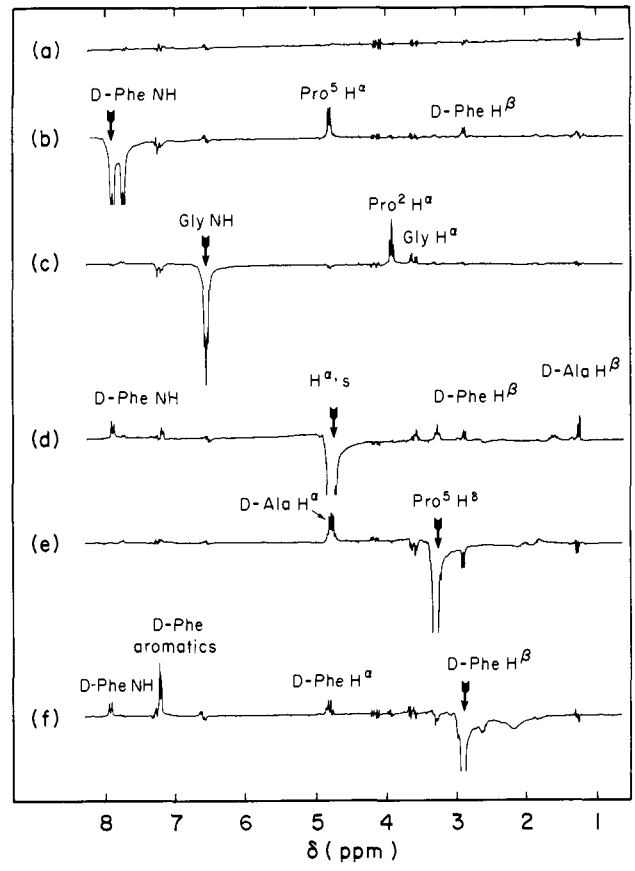

Figure 4. 1-D NOE difference spectra of cyclo(D-Phe-Pro-Gly-D-Ala-Pro) in $CDCl_3$ at 303 K. (a) Null experiment: difference between two off-resonance saturating frequencies; (b) Phe NH saturated; (c) Gly NH saturated; (d) Pro-5 H^α, Phe H^α, Ala H^α saturated; (e) Pro-5 H^β saturated; and (f) Phe H^β saturated.

Table IV. Summary of Distances Obtained from 1-D and 2-D NOE Experiments[h]

spin *i*	spin *j*	1-D σ_{ij}	2-D σ_{ij}	1-D r_{ij}	2-D r_{ij}	X-ray r_{ij}
methylene H_A	methylene H_B	0.51[a]	*b*	1.75[a]	*b*	1.65
Pro-2 H^α	Gly NH	0.18	0.15	2.10	2.15[c]	2.16
upfield Gly H^α	Gly NH	0.09	*b*	2.35	*b*	2.24
Ala NH	Gly NH	*b*	0.04	*b*	2.70[d]	2.65
Phe NH	Pro-5 H^α	0.08	*b*	2.40	*b*	2.40
Pro-5 H^δ	Ala H^α	0.07	0.08	2.45	2.40[c]	2.29, 2.93[e]
downfield Pro-2 H^δ	Phe H^α	*b*	0.08	*b*	2.40[d]	2.01
upfield Pro-2 H^δ	Phe aromatics	0.02	*b*	3.00[c]	*b*	3.26, 4.49[f]
Phe H^δ	Phe aromatics	0.06	0.06	2.50[c]	2.50[d]	2.50, 2.56[g]

[a] Average of σ_{ij} for three interactions between nonequivalent methylene protons. 1.75 Å is used as the distance between two methylene protons. [b] Not measured. [c] Uncertainty ±0.2 Å. [d] Uncertainty ±0.3 Å. [e] The Pro-5 H^δ methylene protons are overlapped in the proton spectrum. Hence, the interaction between D-Ala H^α and Pro-5 H^δ represents the total effect from both methylene protons. The X-ray distances represents the distances to each of the methylene protons. [f] As in footnote *e*, spectral overlap prevents the observance of each aromatic proton individually. The X-ray distances represents the distances from the upfield Pro-2 H^δ to each of the ortho aromatic protons. [g] X-ray distances represent the two shortest distances from the two D-Phe β protons to the two *ortho* aromatic protons. [h] Uncertainty ±0.1 Å except as noted.

resonances are saturated simultaneously, many Overhauser effects are observed. There is a strong interaction between one of the α-protons and Phe NH (9%). As discussed previously, this interaction must be between Pro-5 H^α and Phe NH and is indicative of a γ turn. There is an NOE (7%) between one of the α-protons and one of the δ-protons of Pro-2 (the downfield resonance) and a weaker NOE (4%) between one of the α-protons and both δ-protons of Pro-5. Which α-proton is involved in each case cannot be determined from this experiment since all three α-protons are saturated simultaneously. However, when both Pro-5 δ-protons are saturated, the difference spectrum shows a multiplet which can be identified unambiguously as Ala H^α by comparison to the 2-D *J*-resolved cross section corresponding to Ala H^α shown in Figure 3. Similarly, saturation of the downfield Pro-2 δ-resonance reveals a multiplet which can be identified as Phe H^α by comparison to the 2-D *J*-resolved cross section. Although the 1-D steady-state NOE experiments only revealed an NOE between Phe H^α and the downfield Pro-2 δ-resonance, a weak NOE was observed between Phe H^α and the upfield Pro-2 δ-resonance in the 2-D NOE spectrum. The Overhauser effects observed in Phe H^α and Ala H^α upon saturation of Pro-2 H^δ (12%) and Pro-5 H^δ (21%) are the largest effects observed between residues 1 and 2 and between residues 4 and 5, respectively. This indicates that the shortest distance between these residues is from the δ-proton of each proline ring to the α-proton of the preceding amino acid.

There is a weak NOE (2%) between the α-proton of phenylalanine and the Phe ring proton. However, only some of the ring protons show an effect. These probably correspond to the ortho protons, since these are the closest to the rest of the amino acid. There is a larger NOE (10%) observed in these aromatic protons when the β-protons are saturated. Hence, the ortho ring protons must be closer to the β-protons than to the α-proton of Phe. When the aromatic protons are saturated, a weak NOE (2%) is observed in the upfield Pro-2 H^δ resonance. This indicates that the aromatic ring is oriented above the proline ring of residue 2. This orientation of the aromatic ring is consistent with the large chemical shift difference observed between the two Pro-2 δ-protons, and it appears to reflect a solution side chain rotamer distribution which favors the same rotamer seen in crystalline cyclo(D-Phe-Pro-Gly-D-Ala-Pro). Further evidence for the position of the aromatic ring is provided by the joint observations that the ortho ring protons are closer to the upfield Pro-2 δ-proton whereas the Phe α-proton is closer to the downfield Pro-2 δ-proton.

Transient Overhauser Effects. Several of the interactions which showed large steady-state Overhauser effects were studied in more detail by measuring the buildup of the transient NOE as a function of the irradiation time. One interesting interaction is the NOE between Gly NH and Pro-2 H^α within the type II β turn. When Gly NH was saturated, the largest NOE observed was with Pro-2 H^α. Therefore, the two-spin approximation should apply to this interaction. The transient NOE as a function of saturation time is shown for this interaction in Figure 5. As expected from a two-spin approximation, the transient NOE is an exponential that levels off at the steady-state value. Equation 2 was used to calculate σ_{ij} for this interaction, and a value of 0.18 s^{-1} was

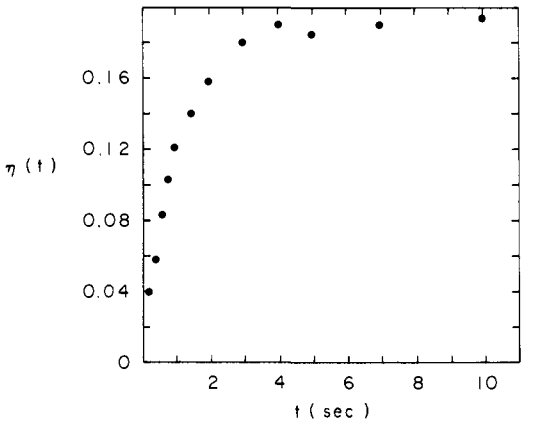

Figure 5. 1-D transient NOE as a function of saturation time: Gly NH saturated, Pro-2 H^α observed.

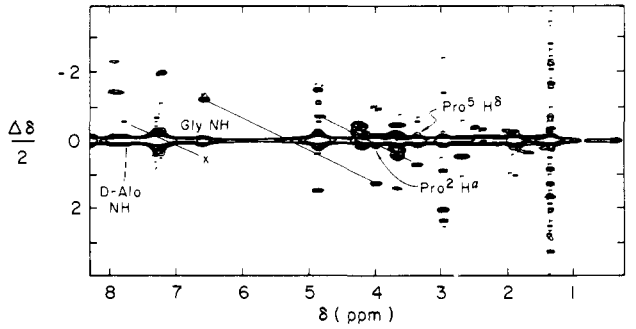

Figure 6. 2-D NOE spectrum of cyclo(D-Phe-Pro-Gly-D-Ala-Pro) in $CDCl_3$. The spectrum was recorded at 303 K with a mixing time of 0.50 s. X denotes a peak which is visible at lower contour levels. An NOE between spins is indicated by a pair of cross-peaks connected by a line, as shown for several representative interactions.

obtained. Several other interactions were analyzed in the same manner to obtain a value of σ_{ij} for each interaction. The distance between methylene protons is known to be 1.75 Å.[8] Since both Gly α-methylene protons and Pro-2 δ-methylene protons are nonequivalent, the transient NOE between methylene protons can be measured for both interactions. If the average value of σ_{ij} for these interactions is assumed to correspond to a distance of 1.75 Å, all other distances can be calculated from eq 3. These results are summarized in Table IV. Interproton distances that were obtained from transient 1-D NOE experiments have an uncertainty of ±0.1 to ±0.2 Å.

2-D NOE Results. Figure 6 shows the 2-D NOE spectrum of cyclo(D-Phe-Pro-Gly-D-Ala-Pro) recorded with a mixing time of 0.50 s. Representative lines are drawn connecting spins related by an NOE. The mixing time of 0.50 s is long enough so that *J* cross-peaks do not appear in this spectrum and only true Overhauser effects are observed.[36] The 2-D NOE spectrum shows all the same effects observed in the steady-state 1-D NOE spectra.

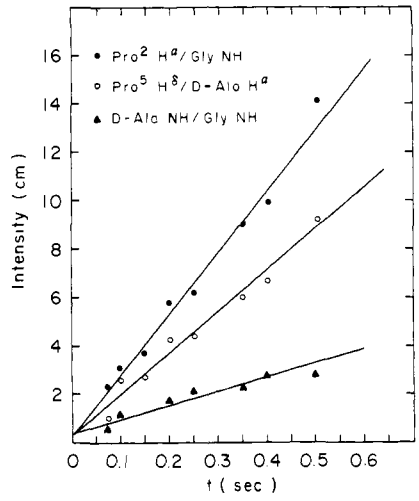

Figure 7. 2-D NOE cross-peak heights as a function of mixing time for the three interactions shown in Figure 6. In all cases, cross sections were taken through the chemical shift of spin i. The following interactions are shown: spin i = Pro-2 H^{α}, spin j = Gly NH; spin i = Pro-5 H^{δ}, spin j = D-Ala H^{α}; spin i = D-Ala NH, spin j = Gly NH.

For example, there is a strong NOE between Gly NH and Pro-2 H^{α}, a weak NOE between Gly NH and the upfield Gly H^{α} resonance, and no effect between Gly NH and the downfield Gly H^{α} resonance. In addition, the 2-D NOE spectrum shows an NOE between Phe H^{α} and each of the Pro-2 δ-protons, whereas the 1-D NOE difference spectrum only shows an NOE between Phe H^{α} and the downfield Pro-2 δ-proton.

The conformation indicated by the NOE data implies a short distance between Phe NH and Ala NH, and an NOE is expected between these two amide protons. However, the existence of such an NOE cannot be confirmed or denied from either the 1-D or 2-D NOE data because the chemical shifts of these two amide protons are too close (0.16 ppm). The two protons cannot be selectively irradiated in a 1-D NOE experiment, and the predicted locations of 2-D NOE cross-peaks between these amide protons are too close to the diagonal to be detected unambiguously. Higher field or phase-sensitive 2-D NOE spectra might overcome this obstacle.

2-D NOE spectra were recorded with several different mixing times, and the initial buildup rate of the NOE was measured for some of the interactions. The initial buildup rates were determined from cross-peak heights measured from cross sections taken through the chemical shifts of the observed protons. Some examples are shown in Figure 7. The buildup rates are linear as expected, and the slopes can be obtained from linear least-squares analysis. For a given interaction, σ_{ij} is this slope divided by the diagonal peak height at $\tau_m = 0$. In practice, there was much scatter in the diagonal peak heights, and an average of short mixing time diagonal peak heights was used for the peak height at $\tau_m = 0$. The 2-D buildup rate of the NOE between two methylene protons could not be measured because of interference from J cross-peaks caused by J coupling.[17,36] Consequently, the 2-D values from cross-relaxation parameters were compared to the 1-D value of 0.51 between two methylene protons which are separated by a distance of 1.75 Å. Interproton distances were calculated from eq 3 and 4 for those interactions whose 2-D NOE buildup rate could be measured. These results are summarized in Table IV. Interproton distances were obtained from 2-D NOE buildup rates of cross-peak heights that have uncertainties of ±0.2 to ±0.3 Å.

Cross-peak heights measured from cross sections provide rather crude estimates of the actual cross-peak intensities. Since the transformed spectrum of any 2-D NOE experiment describes a three-dimensional surface, an integrated peak volume is required to describe completely the intensity of a cross-peak in a 2-D NOE spectrum. Since the software is not generally available to compute the integrated volume of a peak, peak heights are typically used as estimates of the intensities. However, the use of peak heights overestimates narrow peaks and underestimates broad peaks.[17] Since broadening occurs in both dimensions as a result of unresolved fine structure, this can result in a large systematic error. We tried to approximate the peak volume by the product of the peak height and the area of a contour taken at half-height. Due to practical limitations, these contours could not be plotted on a scale large enough to allow precise measurement of the contour areas. Consequently, meaningful buildup rates could not be determined from cross-peak volumes in most cases due to the large random error associated with the measurement of contour areas.

As discussed above, the use of peak heights as a measure of intensity can result in large systematic error in the peak intensities. These intensities can be further distorted by the use of a sine-bell or other resolution enhancement window function in combination with poor digital resolution. However, these problems are not as serious as they may seem initially since only relative intensities are needed. Since diagonal and off-diagonal peaks are treated equally, this error is minimized. Also, the r_{ij} dependence of σ_{ij} means that the percent error associated with r_{ij} is $^1/_6$ the percent error associated with σ_{ij}. Hence, the error in the interproton distances is significantly less than the error associated with the peak intensities.

Comparison of 1-D and 2-D NOE Results. There is excellent agreement between the results obtained from 1-D and 2-D NOE spectra. The same Overhauser effects are observed, and there is excellent agreement between the interproton distances obtained by the two methods. The error associated with the interproton distances is the same for both methods.

The major advantage of 2-D NOE experiments over 1-D NOE double resonance experiments is that 2-D NOE experiments do not require a second resonance frequency. Hence, 2-D NOE spectroscopy does not have the problems caused by the need to irradiate selectively one resonance without affecting neighboring resonances. The lack of complete selectivity in 1-D NOE double resonance experiments can cause serious problems for interpretation in a crowded spectrum. 2-D NOE spectroscopy is also better for observing weak interactions. In 1-D NOE difference spectra, small Overhauser effects can be obscured by small dispersion mode peaks caused by Bloch–Siegert shifts and subtraction artifacts.[28] A more practical advantage of 2-D NOE spectroscopy is that the entire network of Overhauser effects in a molecule is seen in a single experiment. A separate 1-D NOE experiment must be performed for each interaction to be studied. Consequently, 2-D NOE spectroscopy is more practical in a multispin system with many interactions.

There are two disadvantages of 2-D NOE spectroscopy as compared to 1-D NOE spectroscopy. The 2-D NOE spectrum is complicated by the existence of J cross-peaks,[31] but these J peaks can be removed if desired.[32,33] The other disadvantage is due to practical limitations associated with the 2-D NOE experiment. A multiplet indicative of a particular proton is easily seen in a 1-D NOE difference spectrum even when this multiplet is overlapped with multiplets from other protons in the normal spectrum. Consequently, an observed interaction in a 1-D NOE difference spectrum is easily assigned to a specific proton even in the case of extreme overlap. It is theoretically possible to assign a cross-peak to a specific proton in a 2-D NOE spectrum in the case of overlap since the fine structure associated with a cross-peak is dependent on the coupling constants associated with the observed proton. However, this is not always possible in practice since poor digital resolution and the calculation of an absolute value spectrum combine to obscure the fine structure associated with the cross-peaks. This situation could be improved through the use of a pure absorption spectrum[37] and better digital resolution, but the resolution in any 2-D NOE spectrum will probably be worse than in a 1-D NOE difference spectrum due to practical considerations

(36) Nagayama, K.; Bachmann, P.; Wüthrich, K.; Ernst, R. R. *J. Magn. Reson.* **1978**, *31*, 133.

(37) States, D. J.; Haberkorn, R. A.; Ruben, D. J. *J. Magn. Reson.* **1982**, *48*, 286.

such as acquisition time and disk storage space. In most cases, the assignment of a cross-peak in a 2-D NOE spectrum can be made from prior knowledge of likely interactions, but ambiguities sometimes result. For instance, the interaction between Phe NH and Pro-5 H^{α} can be seen in the 2-D NOE spectrum, but the 2-D NOE spectrum does not allow the cross-peak to be assigned to Pro-5 H^{α} as opposed to Phe H^{α}. In general, 1-D and 2-D NOE spectroscopy provide consistent and complementary information.

Comparison of Solution and Crystal Interproton Distances. Distances between protons calculated from X-ray derived coordinates for crystalline cyclo(D-Phe-Pro-Gly-D-Ala-Pro) are given in Table IV along with the 1-D and 2-D NOE derived distances. Analysis of these interproton distances serves as an indicator of the consistency of the two structural approaches, and more importantly, it allows a direct comparison of the solution and crystal conformations of this model peptide. There is a remarkable correspondence of the distances from NOE and from X-ray; nearly all are the same within experimental error. Deviations between X-ray and NOE results in two distances involving Pro-2 H^{δ}'s are outside the range of experimental error, and they may reasonably be correlated with a site of conformational change between crystal and solution. In a previous detailed analysis of the proline ring geometries of this cyclic pentapeptide using coupling constants,[19] Pro-2 was found to adopt a different conformational distribution in solution from that in the crystal while Pro-5 was fixed in the same ring geometry in both states. In this previous study, an equilibrium between two oppositely puckered ring conformations was proposed in solution for Pro-2. The present data are consistent with the previous study in indicating a difference between crystal and solution conformations around Pro-2, but they offer no information on the dynamic aspect of the conformational description, except that the Overhauser effects are transmitted to and from Pro-2 despite any conformational averaging.

Conclusions

Quantitative interproton distances in a cyclic pentapeptide were obtained from both 1-D and 2-D NOE buildup rates, and there is excellent agreement between the distances obtained by the two methods. A single correlation time for all protons in this rigid peptide was assumed in all distance calculations, and this assumption is justified by T_1 and NOE results. A two-spin approximation was also used in all distance calculations. This is a good approximation for all interactions studied except between Gly NH and both Gly H^{α} and Ala NH, and between Pro-2 H^{α} and the Phe aromatic ring protons. Consequently, these three interproton distances are only estimates of the actual distances since the two-spin approximation is not strictly valid for these interactions. Nonetheless, striking agreement was observed between interproton distances from NOE and those for the crystal structure of this peptide as solved by X-ray diffraction. Not only does this correspondence indicate that the methods employed in the NOE analysis seem sound, but it also affords a direct comparison of the crystal and solution conformations of a cyclic model peptide. Only in the region of the Pro-2 pyrrolidine ring does there appear to be a significant conformational change in the peptide between the two environments. In both states, the peptide adopts a conformation with two transannular hydrogen bonds, one in a β turn around D-Phe-Pro-2-Gly-D-Ala and the other in a γ turn around D-Ala-Pro-5-Gly. The proximity of Gly NH to Pro-2 H^{α}, which gives rise to a strong NOE, is a hallmark of a type II β turn when accompanied by evidence for a 4–1 intramolecular hydrogen bond as previously found for this peptide.[18] The proximity of Phe NH to Pro-5 H^{α} is definitive evidence for a trans proline, and it is consistent with the presence of a γ turn; additional data previously reported[18] indicated the existence of the 3–1 intramolecular hydrogen bond. The turn is further supported by the (weak) NOE between the Gly NH and the Ala NH. Other conformationally informative NOE's placed the Gly NH with respect to the Gly H^{α}'s and allowed unequivocal assignment of these two methylenes. Furthermore, NOE data supported the preferred rotamer of the Phe ring as over the Pro-2 ring, hence accounting for the widely separated Pro H^{δ} protons.

Acknowledgment. We thank Arlene L. Rockwell for performing the ^{13}C T_1 measurements. L.M.G. is a Fellow of the A.P. Sloan Foundation, 1984–1986. Support from the National Institutes of Health (for the purchase of Burker WM250 and GM 27616 to L.M.G.) is gratefully acknowledged.

Registry No. *cyclo*-(D-Phe-Pro-Gly-D-Ala-Pro), 75929-66-7.

Relative ^{36}S–^{34}S Kinetic Isotope Effects

Piotr Paneth and Wladyslaw Reimschüssel*

Contribution from the Institute of Applied Radiation Chemistry, Technical University (Politechnika) of Lodz, 90-924 Lodz, Poland. *Received July 16, 1984*

Abstract: Two sulfur kinetic isotope effects, k_{32}/k_{34} and k_{32}/k_{36}, were measured for the thermal isomerization of bis(5,5-dimethyl-2-oxo-1,3,2-dioxaphosphorinanyl) sulfide (**1**) to *P*-oxo-*P'*-thionobis(5,5-dimethyl-1,3,2-dioxaphosphorinanyl) oxide (**2**). The *r* value is equal to 1.92 ± 0.11 for the relative ^{36}S–^{34}S kinetic isotope effect and is independent of isotopic composition and solvent used. This value is in the range predicted earlier for carbon and heavier atoms.

It has been 3 decades since Bigeleisen,[1] on the basis of the simple models, predicted that the ^{14}C kinetic isotope effect ($k_{12}/k_{14} - 1$) should be about 2 times larger than the corresponding ^{13}C isotope effects ($k_{12}/k_{13} - 1$). Relative ^{14}C–^{13}C kinetic isotope effects were analyzed in detail by Stern and Vogel.[2] The calculated values were compared with experimental results, and a range 1.8–2.0 for the ratio *r* (eq 1) was obtained. Exceptions to this generalization are usually considered to result from experimental errors,[3] but other explanations such as anomalous temperature dependence[2] or reaction complexity[4] can be encountered.

$$r = \frac{\ln (k_{12}/k_{14})}{\ln (k_{12}/k_{13})} \quad (1)$$

Although some other elements such as oxygen and sulfur have suitable stable isotopes, to the best of our knowledge, there are no data on *r* values for kinetic isotope effects of any heavy atoms except for carbon. An *r* value has been used qualitatively for the comparison of two measured sulfur isotope effects: k_{32}/k_{35} and k_{32}/k_{34}.[5] In order to verify whether the range of *r* values estimated

(1) Bigeleisen, J. *J. Phys. Chem.* **1952**, *56*, 823.
(2) Stern, M. J.; Vogel, P. C. *J. Chem. Phys.* **1971**, *55*, 2007.
(3) Melander, L.; Saunders, W. H., Jr. "Reaction Rates of Isotopic Molecules"; Wiley: New York, 1980.
(4) Paneth, P. *J. Chem. Phys.*, in press.

0002-7863/85/1507-1407$01.50/0